Contribution to the IAEA Coordinated Research Program on Prompt Fission Neutron Emission , October 2013

Prompt-neutron spectra from a general description of the fission process

Karl-Heinz Schmidt[a] and Beatriz Jurado[b]

Abstract: A new semi-empirical model of the fission process is described, which covers most of the properties of the fission fragments and the emitted neutrons and photons in a global and consistent way. The model is based on fragment shells that are deduced from measured fission-fragment mass distributions, assuming that the macroscopic contribution of the compound nucleus and the microscopic contributions of the nascent fragments in the potential-energy surface are separable. The distributions of the collective coordinates are attributed to the motion of the quantum oscillators in their respective potential pockets perpendicular to the fission path. Different contributions to the excitation energies of the final fragments and their division at scission are described with the help of statistical mechanics. Intrinsic excitation energies of the fragments at scission are consistently described together with the even-odd effect in fission-fragment *Z* distributions. Mass-dependent equilibrium deformations of the nascent fragments are adjusted to measured average prompt-neutron multiplicities. A unique set of parameters is found, which reproduces a large variety of measured data for all heavy fissioning systems with a good precision. In contrast to most available models, this approach is applicable to fissioning systems, for which no experimental data are available.

Introduction

Global parametrisations and very elaborate models have been developed for calculating the energy spectra of prompt fission neutrons and their multiplicity distributions. Most of them are based on measured mass-TKE distributions of the fission fragments. With the help of the Q values for specific nuclear-charge and mass splits and by considering the initial excitation energy, the total excitation energy TXE of the fragments can directly be deduced. With an assumption on the division of the TXE between the fragments, which needs to be consistent with the observed mass-dependent neutron multiplicities, the initial conditions of both fragments for a statistical de-excitation code of the Weisskopf or Hauser-Feshbach type are determined.

The task is appreciably more difficult when this experimental basis, the measured mass-TKE distribution, is not available. In this case, this information must be provided by a model calculation. The GEF code has been developed for this purpose. It is a semi-empirical model of the fission process, which covers most of the properties of the fission fragments and the emitted neutrons and photons in a global and consistent way. In addition to the mass-TKE distribution it also calculates the division of the TXE between the fragments and the angular momenta of the fragments. Moreover, the specific initial conditions of each individual fragment are given. This report gives an overview on the underlying physics ideas and the general technical features of the code and presents some results. More detailed information on the code can be found in the report JEF/DOC 1423 [[1]]. The final aim of the present work is to provide predictions for the multiplicities and the energy spectra of the prompt neutrons.

a E-mail: schmidt-erzhausen@t-online.de, URL: http://www.khs-erzhausen.de
b E-mail: jurado@cenbg.in2p3.fr, CENBG, CNRS/IN2 P3, Chemin du Solarium B.P. 120, F-33175 Gradignan, France

Fission channels

Experimental systematics

Figure 1 gives an overview on the measured mass and nuclear-charge distributions of fission products from low-energy fission. Fission of target nuclei in the actinide region, mostly induced by neutrons, shows predominantly asymmetric mass splits. A transition to symmetric mass splits is seen around mass 258 in spontaneous fission of fusion residues. Electromagnetic-induced fission of relativistic secondary beams covers the transition from asymmetric to symmetric fission around mass 226 [2]. A pronounced fine structure close to symmetry appears in ^{201}Tl [3] and in ^{180}Hg [4]. It is difficult to observe low-energy fission in this mass range. Thus, ^{201}Tl could only be measured down to 7.3 MeV above the fission barrier due to its low fissility, which explains the filling of the minimum between the two peaks. Only ^{180}Hg was measured at energies close to the barrier after beta decay of ^{180}Tl. Considering the measured energy dependence of the structure for ^{201}Tl [3], the fission characteristics of these two nuclei are rather similar. Also other nuclei in this mass region show similar features, which have been attributed to the influence of fragment shells [5]. These shells are different from those governing the asymmetric fission of the actinides. They are not considered in the present model that concentrates on heavier nuclei with mass numbers A>200, which are more important for technical applications.

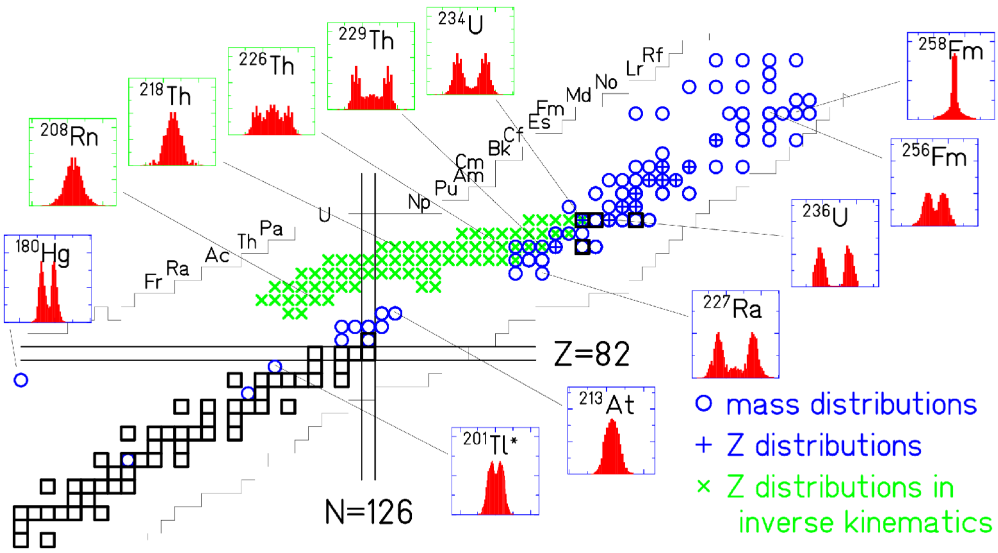

Figure 1. General view on the systems for which mass or nuclear-charge distributions have been measured. The distributions are shown for 12 selected systems. Blue circles (blue crosses): Mass (nuclear-charge) distributions, measured in conventional experiments [3, 4], and references given in [2]. Green crosses: Nuclear-charge distributions, measured in inverse kinematics [2].

Size of the heavy fragment in asymmetric fission

In the range where asymmetric fission prevails, e.g. from ^{227}Ra to ^{256}Fm, the light and the heavy fission-product components gradually approach each other, see figure 1. A quantitative analysis reveals that the mean mass of the heavy component stays approximately constant [6] at about A=140. This has been explained by the influence of a deformed ($\beta \approx 0.6$) fragment shell at N=88 and the spherical shell at N=82 [7], suggesting that the position of the heavy fragment is essentially constant in neutron number.

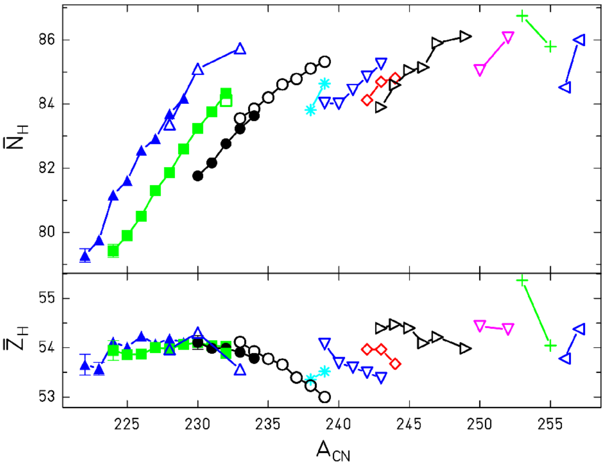

Figure 2. *Mean neutron and proton number of the heavy component in asymmetric fission in the actinide region before the emission of prompt neutrons. The values were deduced from measured mass and nuclear-charge distributions using the semi-empirical GEF code [8] for the correction of charge polarization and prompt-neutron emission. Open symbols denote results from conventional experiments, full symbols refer to an experiment with relativistic projectile fragments of ^{238}U [2]. Data points for the same Z_{CN} are connected (See [8] for references of the underlying experimental data.)*

New data on Z distributions over long isotopic chains [2], however, reveal very clearly that the position in neutron number varies systematically over more than 7 units, while the position in proton number is approximately constant at Z=54, see figure 2. The rather short isotopic sequences covered in former experiments did not show this feature clearly enough and gave the false impression of a constant position in mass.
This finding represents a severe puzzle to theory, since shell-model calculations do not show any shell stabilization near Z=54 at $\beta\approx0.6$ [7,[9]].

Separability principle

The microscopic-macroscopic approach has proven to be very useful for calculating nuclear properties, in particular in applications to fission [[10]]. The early influence of fragment shells on the fission path, deduced from two-centre shell-model calculations [[11]], makes its application to fission even more powerful. It means that the microscopic properties of the fission observables are essentially determined by the shells of the fragments, and only the macroscopic properties are specific to the fissioning system [[12]].
This "separability principle" was exploited in the GEF code [8], which relies on an empirical description of the macroscopic stiffness parameters in the relevant normal modes and empirically deduced fragment shells, which are valid for all fissioning systems. Figure 3 demonstrates that the mass distributions over a large range of systems can be described very well with the same parameter set. For a more complete overview see ref. [1].

Dynamical effects

Statistical scission-point models, e.g. refs. [7,[13]], suffer from the neglect of dynamical effects. Stochastic calculations revealed that, depending on the nature of the collective degree of freedom, dynamical effects induce a kind of memory on the fission trajectory, which may be accounted for by an early freeze-out that depends on the influence of inertia. Mass-asymmetric distortions have a large inertia, and thus the mass distribution is already essentially determined slightly behind the outer fission saddle [[14]]. Charge polarization has a small inertia, and the distribution is determined close to scission [[15]].

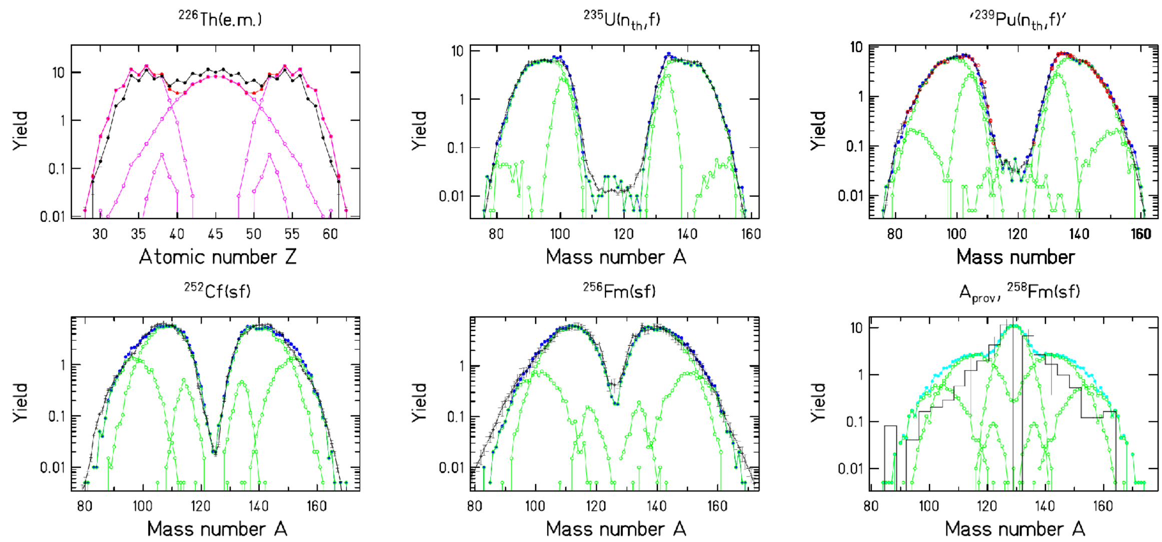

Figure 3. *Nuclear-charge and post-neutron mass distributions of fission fragments. (For ^{258}Fm(sf) the "provisional mass" A_{prov} is shown, which is directly deduced from the ratio of the kinetic energies of the fragments and thus not corrected for neutron emission.) Experimental or evaluated data (black lines, respectively histogram) for electromagnetic-induced (e.m.), thermal-neutron-induced (n_{th},f) and spontaneous fission (sf) are compared with predictions of the GEF code [8] (red and green lines). The red symbols for ^{239}Pu(n_{th},f) show the experimental data behind the evaluation. The contributions of different fission channels are shown. (See [8] for references of the data.)*

Fluctuations

Most fission observables form bell-shaped distributions around a mean value. This suggests treating the corresponding collective degree of freedom as an harmonic quantum oscillator coupled to a heat bath of temperature *T*. Especially for the charge-polarization degree of freedom there is a long discussion about the importance of the zero-point motion [16, 17]. Nix estimated the level spacing in the oscillator corresponding to mass-asymmetric distortions at saddle with the liquid-drop model to 1-2 MeV in the actinide region [18]. According to the smaller widths of the corresponding components to the mass distribution, the level spacing for oscillations in the two asymmetric fission valleys (Standard 2 and Standard 1) is expected to be even larger. Also for oscillations in the charge-polarization degree of freedom, the level spacing is in the order of 10 MeV. This values are appreciably larger than the temperature values of actinides, which are about 0.5 MeV in the constant-temperature regime [19]. Thus, in a statistical approach the charge-polarization degrees of freedom is essentially not excited, and also the widths of the fission channels in mass asymmetry are expected to be strongly influenced by the zero-point motion in low-energy fission.

Also the angular-momentum distributions of the fragments have been explained by "orientation pumping" due to the uncertainty principle [20]. Experimental indications for thermal excitations of spherical fragments [21] have also been explained by the compensation of the orbital angular momentum, which itself is induced by the zero-point motion [22]. Here it is the operator of the orbital angular momentum which does not commute with the angle that characterizes the direction of particle motion. Thus, all fragment angular momenta measured in low-energy fission [23] are explained by the quantum-mechanical uncertainty principle. There is no room for excitations of the angular-momentum-bearing modes [24].

Due to the strong influence of quantum-mechanical effects it is mandatory to explicitly consider these effects, as it is e.g. done in the self-consistent microscopic approach of ref. [25]. Stochastic approaches with classical models [26] may miss certain aspects of the fission dynamics..

Comparison with previous ideas

Several descriptions of the fission observables with applications of the statistical model have been proposed in the past. The present approach is rather close to the outline of a scenario proposed by Jensen and Døssing [27], although the present model covers a larger variety of observables. More importantly, it also tries to better exploit available empirical information.

Jensen and Døssing presented a statistical calculation of the mass distribution in fission with some ideas about the dynamics of the process. The most important modifications applied in the GEF code are: (i) The shell effects that were calculated from single-particle energy spectra in a Woods-Saxon potential with the Strutinsky method in ref. [27] are replaced by global fragment shells, which are adjusted to the measured mass distributions. The separability principle simplifies this task considerably, since the fragment shells are assumed to depend only on the fragment, and, thus, they are the same for all fissioning systems. (ii) The nuclear level density that was calculated from the same single-particle spectrum including pairing correlations using the BCS approximation in ref. [27] is replaced by an empirical constant-temperature formula [19], which seems to be in good agreement with recent experimental results [28]. (iii) The influence of quantum-mechanics, in particular the zero-point motion, has been considered to model the distributions of collective coordinates. They are attributed to the motion of the quantum oscillators in their respective potential pockets perpendicular to the fission path. The parameters of these oscillators are deduced from experimental data. In addition, the shapes of the fragments at scission, the charge polarization, the angular momenta, and other properties of the fragments are calculated on the basis of similar ideas.

Prompt-neutron yields

Transformation of energy – the different contributions

In low-energy fission, the Q value of the reaction ends up either in the total kinetic energy (TKE) or the total excitation energy (TXE) of the fragments. The TKE is closely related to the distance of the centres of the two nascent fragments at scission, but, even if the pre-scission kinetic energy is neglected, it cannot give information on the shapes of the individual fragments. The TXE, however, can be attributed to the individual fragments by a kinematical measurement of the prompt-neutrons. Still, there is no direct experimental information available on the processes, which are responsible for the transformation of part of the Q value into the excitation energies of the separated fragments. The situation is schematically illustrated in figure 4. Before scission, dissipation leads to intrinsic excitations, collective modes perpendicular to the fission direction ("normal modes" [18]) may be excited, and, finally, some energy is stored in deformation of the nascent fragments that is induced by the Coulomb repulsion. The remaining part is found as pre-scission kinetic energy [29]. After scission, collective excitations and deformation energy are transformed and add up to the intrinsic excitations of the separated fragments.

The situation at scission is important for the understanding of fission dynamics, e.g. the magnitude of dissipation and the coupling between the different collective degrees of freedom, but without additional information, the repartition of the different contributions between the fragments remains ambiguous.

Origin of the saw-tooth shape

There is widespread agreement that the saw-tooth shape of the prompt-neutron yields, see figure 5, is caused by the deformation energies of the nascent fragments at scission. The scission-point model of ref. [7] attributes it to the influence of fragment shells, the random-neck-rupture model [30] links it to the location of the rupture, and also microscopic calculations predict large deformation energies of the fragments near scission [31]. Large even-odd effects in the fragment Z distributions indicate that the intrinsic excitation energy at scission is generally much too low to account for the variation of the prompt-neutron yield by several units over the different fragments.

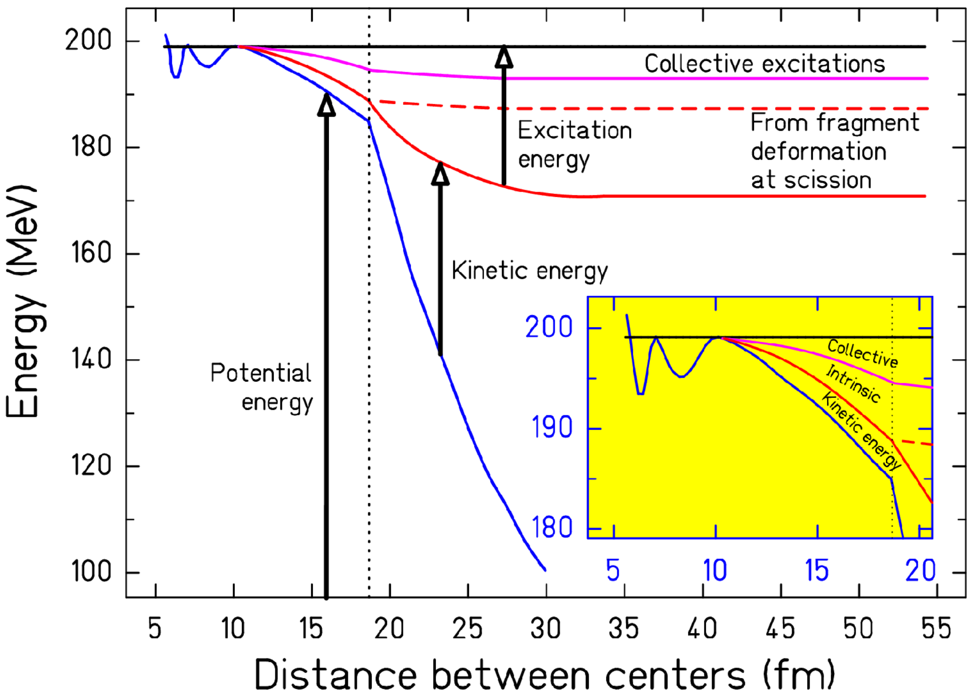

Figure 4. Schematic drawing of the transformation of energy during the fission process of ^{236}U with an initial excitation energy equal to the height of the fission barrier.

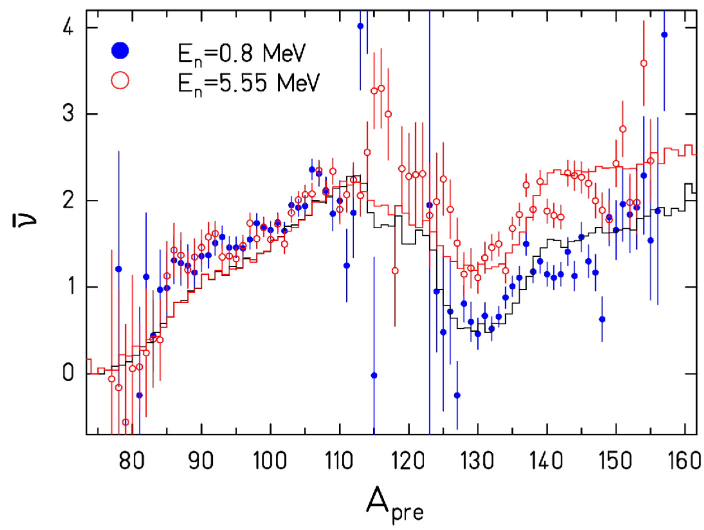

Figure 5. *Measured prompt-neutron yield in $^{237}Np(n,f)$ as a function of pre-neutron mass at two different incident-neutron energies [32] (data points) in comparison with the result of the GEF code [8] (histograms).*

Differential behaviour – energy sorting

Recent experimental results reveal that nuclei exhibit an essentially constant temperature, may be up to excitation energies of 20 MeV [33] with a temperature parameter that is grossly proportional to $A^{-2/3}$ [19]. This behaviour is explained by the breaking of pairs in the so-called superfluid regime [34]. This leads to a considerable increase of the heat capacity [35] and consequently to a slow variation of temperature as a function of excitation energy. Note that the BCS approximation severely underestimates the pairing condensation energy and consequently also the magnitude of the heat capacity in the so-called superfluid regime [36]. Thus, the assumption of a constant nuclear temperature becomes a good approximation. This implies that the intrinsic excitation energy of the two nascent fragments at scission is subject to energy sorting [37, 38, 39]: The hotter light fragment transfers essentially all its intrinsic excitation energy to the colder heavy fragment. This energy sorting manifests itself in the mass-dependent neutron yields. Fig. 5 shows data for neutron-induced fission of ^{237}Np with E_n = 0.8 MeV and E_n = 5.55 MeV as an example. The additional initial energy leads to an increased neutron yield from the heavy fragments, only. The behaviour is well reproduced by the GEF code, which includes a model for the process of energy sorting.

Even-odd effect in Z yields

Experimental systematics

A systematic view on the local even-odd effect in fission-fragment *Z* distributions [40] reveals a regular pattern and a general dependence on the fissioning system, see figure 6. The magnitude of the even-odd effect is small at symmetry, and it increases strongly with increasing asymmetry. At the same time, the even-odd effect generally decreases for heavier systems. The even-odd effect in the light fragment group of nearby even-*Z* and odd-*Z* systems is essentially identical, except at symmetry, where the even-odd effect in odd-*Z* systems is exactly zero. Electromagnetic excitations lead to slightly higher excitation energies, thus reducing the magnitude of the even-odd effect. The large number of systems investigated revealed that the appearance of a large even-odd effect at large asymmetry is a general phenomenon, also in odd-Z fissioning systems [41]. In any case, there is an enhancement of even-Z fragments in the light fragment group, indicating that it is the enhanced production of even-Z light fragments in their ground state, which is at the origin of the large even-odd effect at extreme asymmetry.

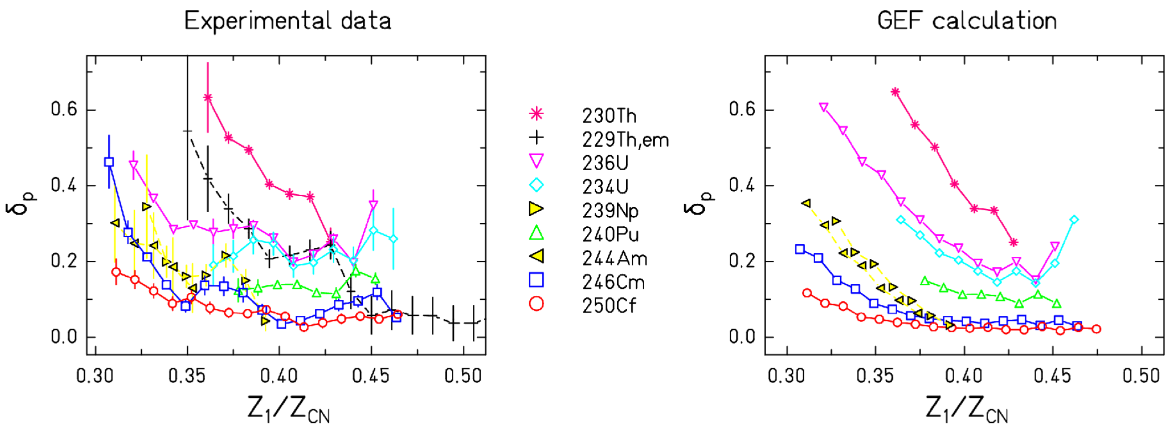

Figure 6. *Measured (left) and calculated (right) local even-odd effect in fission-fragment Z distributions in (n_{th},f) reactions. The fissioning nuclei are indicated. Data for fission of ^{229}Th, induced by electromagnetic excitations are included. See ref. [40] for references of the data.*

Final stage of energy sorting

It seems straightforward to attribute the enhanced production of even-*Z* light fragments to the energy-sorting mechanism [42] that explained already the differential behaviour of the prompt-neutron yields. If the time until scission is sufficient for the energy sorting to be accomplished, the system can still gain an additional amount of entropy by predominantly producing even-even light fragments. Compared to the production of odd-odd light fragments, the excitation energy of the heavy fragment increases by two times the pairing gap, and its entropy increases due to the increasing number of available states in the heavy fragment. The right part of figure 6 shows a calculation with the GEF code, where this idea is included in a schematic way. The basic features are: (i) The excitation energy induced by dissipation grows with the Coulomb parameter $Z^2/A^{1/3}$, and the time needed for complete energy sorting is correspondingly increased. Also the energy gain from saddle to scission increases, and, thus the energy exceeds the constant-temperature domain. This explains the observed reduction of the even-odd effect for heavier systems. (ii) The temperature difference of the nascent fragments grows with increasing asymmetry, which enhances the energy-sorting process. This explains the strong increase of the even-odd effect at large asymmetry.

Charge polarization

Experimental information

Most experimental information on charge polarization at scission is indirect, because only the fragment masses after the emission of prompt neutrons can be measured with good resolution. Thus, the influence of prompt-neutron emission has to be corrected. This correction introduces some uncertainties, because most data on mass-dependent prompt-neutron multiplicities are not very precise, and for many systems such data are not available.

Figure 7 shows the measured deviation of the mean nuclear charge from the UCD (unchanged charge distribution) value for a fixed post-neutron mass and the standard deviation of the corresponding nuclear-charge distribution for the thermal-neutron-induced fission of ^{235}U [43]. The influence of the even-odd staggering of the Z yields is clearly visible in both quantities.

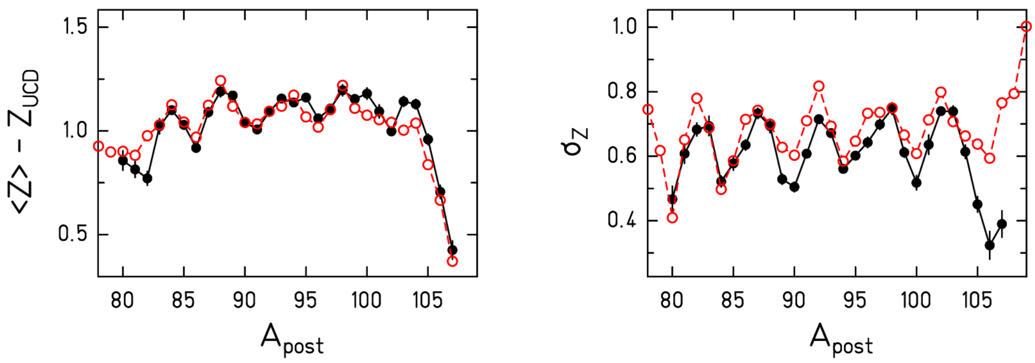

Figure 7. *Indirect information on the charge polarization in $^{235}U(n_{th},f)$. Left part:Deviation of the mean nuclear charge from the UCD (unchanged charge distribution) value for a fixed post-neutron mass A_{post}. Experimental data [43] (full points) are compared with the result of the GEF code [8] (open points). Right part: Standard deviation of the nuclear-charge distribution for a fixed post-neutron mass A_{post}. Experimental data [43] (full points) are compared with the result of the GEF code [8] (open points).*

Simulation

The simulation of the nuclear-charge distributions for fixed post-neutron mass starts from the calculated pre-neutron nuclide distribution and the excitation energy of each individual fragment. The emission of prompt neutrons must be considered, which is constrained by measured mass-dependent prompt-neutron multiplicity distributions. The good agreement with post-neutron fragment distributions shown in figure 7 was obtained by minimizing the potential energy of the scission configuration, approximated by quadrupole-deformed fragments with a tip distance of 1 fm with respect to their N/Z ratios. However, for the asymmetric fission channels, the value of $<Z>-Z_{UCD}$ had to be increased (decreased) by 0.3 units in the light (heavy) fragment. This additional charge polarization may be attributed to the influence of the shell effects. The mean deformation of the fragments at scission is linked to the mean prompt-neutron multiplicity, considering the amount of intrinsic excitation energy at scission, which is consistent with the description of the even-odd effect in the *Z* distributions.

Fragment kinetic energies

In the GEF code, the total kinetic energy of the fission fragments is given by subtracting the total excitation energy of the separated fragments from the sum of the initial excitation energy of the fissioning nucleus and the Q value of the fission process. The resulting distribution for $^{235}U(n_{th},f)$ is shown in figure 8. The overall behaviour is in agreement with expectations from systematics. In the model, the shape of the energy distribution for a fixed mass is mainly defined by the distribution of fragment deformations at scission, which is taken as a Gaussian distribution with a maximum in the respective potential minimum. These shapes are assumed to be decisive for the amount of deformation energy of the separated fragments with respect to their respective ground state, which finally adds up to their intrinsic excitation energy. This explains the skewness of the distributions, which seem to be slightly larger than found in experiment.

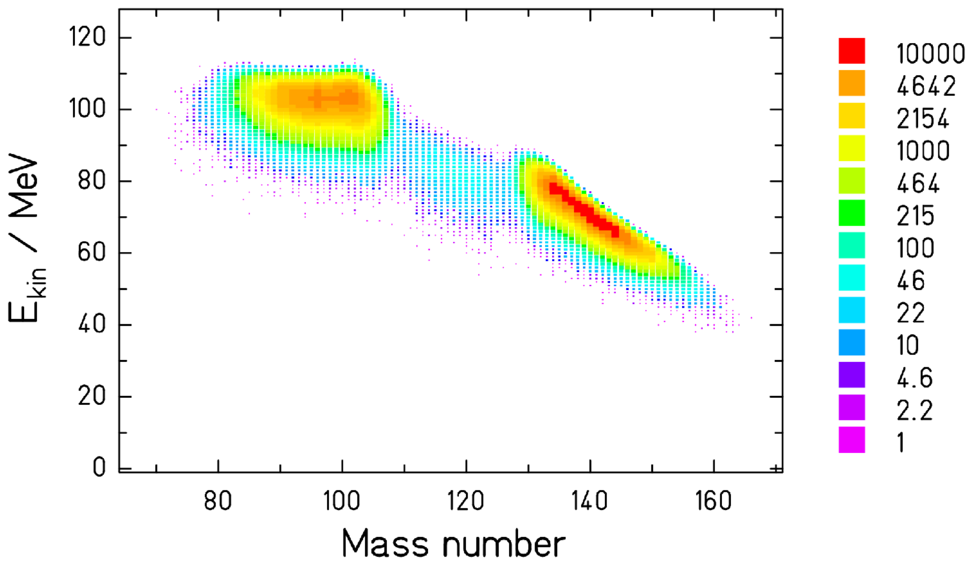

Figure 8. *Two-dimensional distribution of kinetic energies and fission-fragment masses before emission of prompt neutrons for* $^{235}U(n_{th},f)$. *The colour scale refers to the counts of the Monte-Carlo calculation with the GEF code.*

Neutron multiplicities

Besides the mass-dependent mean prompt-neutron yields, see figure 5, there exist two other experimental results, which have been determined with high accuracy: The mass-integrated neutron-multiplicity distribution and the mean number of prompt fission neutrons.
The measured mean number of prompt-fission neutron yields is compared in table 1 with the values given by the GEF code for some selected systems. The same parameter set was used for all systems.

Table 1. *Selected values of mean prompt-neutron multiplicities. The measured values are compared with the result of the GEF code.*

System	E_n	Exp.	GEF
$^{235}U(n,f)$	thermal	2.41 [[44]]	2.39
$^{235}U(n,f)$	0.5 MeV	2.46 [[45]]	2.51
$^{235}U(n,f)$	5.55 MeV	3.19 [45]	3.29
$^{237}Np(n,f)$	0.8 MeV	2.73 [32]	2.57
$^{237}Np(n,f)$	5.55 MeV	3.46 [32]	3.33
$^{239}Pu(n,f)$	thermal	2.88 [44]	3.02
$^{252}Cf(sf)$	---	3.77 [[46]]	3.66

Figure 9 demonstrates the good agreement of the calculated neutron-multiplicity distributions for $^{235}U(n_{th},f)$ and $^{239}Pu(n_{th},f)$ with the experimental data. Like in the case of the fragment kinetic energies, the width is mostly caused by the distribution of fragment deformations at scission. The shape of the distribution is well reproduced for all three systems.

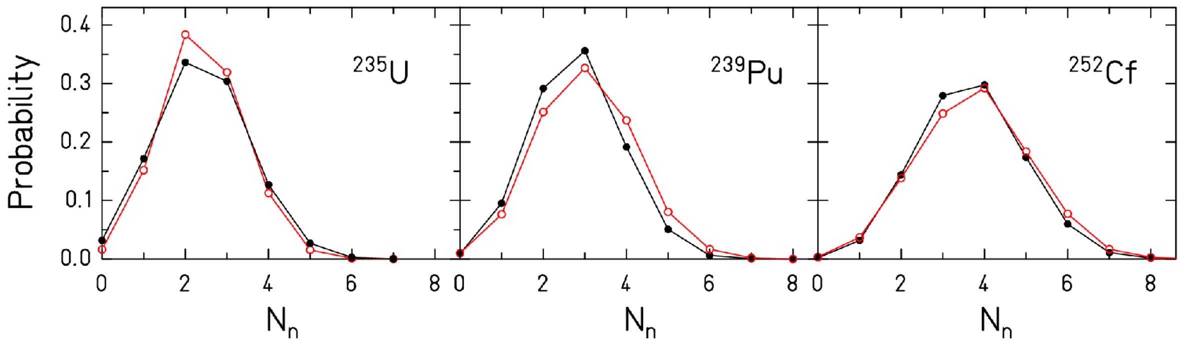

Figure 9. *Measured prompt-neutron multiplicity distributions [44,46] for $^{235}U(n_{th},f)$ (left part), $^{239}Pu(n_{th},f)$ (middle part) and $^{252}Cf(sf)$ (right part) are compared to the results of the GEF code (open symbols).*

Prompt-neutron spectrum

The experimental prompt-fission-neutron spectra for the systems $^{235}U(n_{th},f)$ [[47]] and $^{252}Cf(sf)$ [[48]] are compared with results of the GEF code in figure 10. In order to better visualize the deviations, the lower panels show a reduced presentation with the spectra normalized to a Maxwellian distribution with the parameter $T = 1.32$ MeV.

In this calculation, the de-excitation of the separated fragments has been obtained within the statistical model. It is assumed that both the emission of neutrons and the emission of E1 gammas does not change the angular momentum on the average, which seems to be a good approximation in the relevant angular-momentum range [[49]]. When the yrast line is reached, the angular momentum is carried away by a cascade of E2 gammas. A constant inverse neutron absorption cross section has been assumed. Gamma competition at energies above the neutron separation energy was considered. The gamma strength of the giant dipole resonance (GDR) following the description proposed in ref. [[50]] was applied. The nuclear level density was modelled by the constant-temperature description of v. Egidy and Bucurescu [[51]] at low energies. The level density was smoothly joined at higher energies with the modified Fermi-gas description of Ignatyuk et al. [52, 53] for the nuclear-state density:

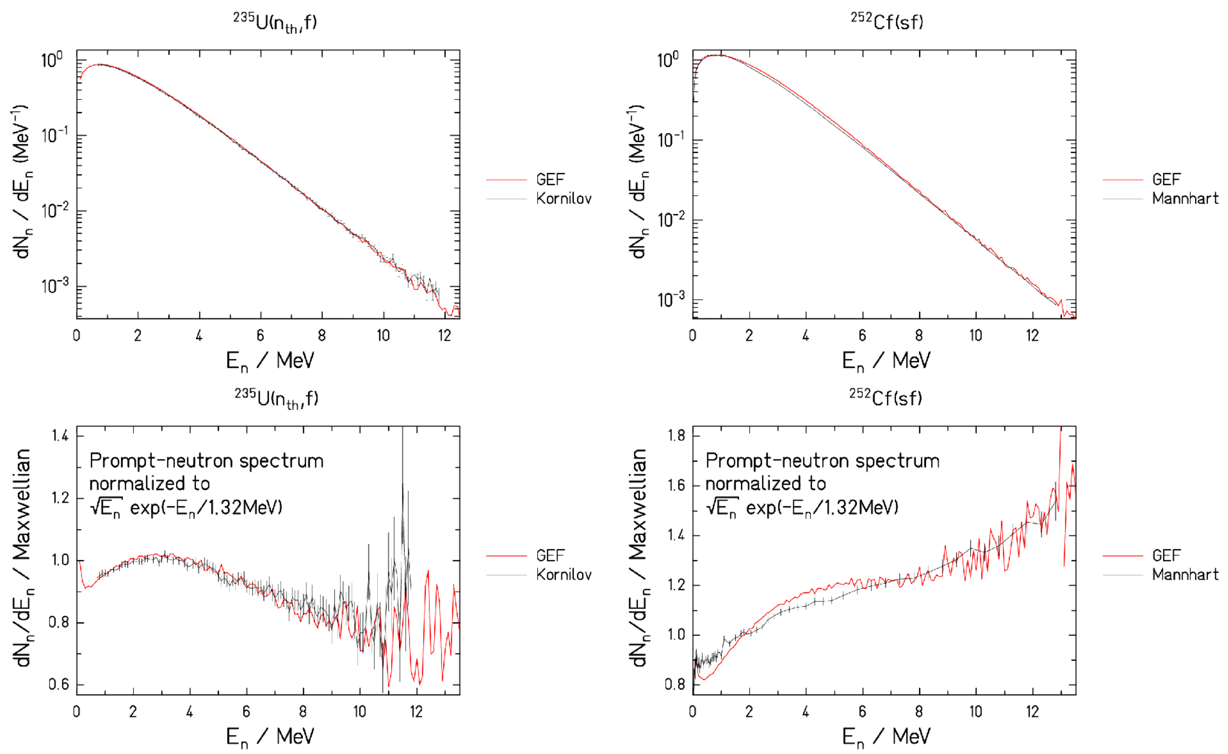

Figure 10. *Experimental prompt-fission-neutron spectra (black lines and error bars) for $^{235}U(n_{th},f)$ [47] (left panels) and $^{252}Cf(sf)$ [48] (right panels) in comparison with the result of the GEF code (red lines) in logarithmic scale. In the lowest panels, all spectra have been normalized to a Maxwellian with T = 1.32 MeV.*

$$\omega \propto \frac{\sqrt{\pi}}{12\tilde{a}^{1/4}U^{5/4}}\exp(2\sqrt{\tilde{a}U})$$

with $U = E + E_{cond} + \delta U(1-\exp(-\gamma E))$, $\gamma = 0.055$ and the asymptotic level-density parameter $\tilde{a} = 0.078A + 0.115A^{2/3}$. The shift parameter E_{cond} represents the pairing-condensation energy given by $E_{cond} = -2\,MeV - n\Delta_0$, $\Delta_0 = \frac{12}{\sqrt{A}}$ with n = 0,1,2 for odd-odd, odd-A and even-even nuclei, respectively, as proposed in ref. [54]. δU is the ground-state shell correction. A constant spin-cutoff parameter was used. The matching energy is determined from the matching condition (continuous level-density values and derivatives of the constant-temperature and the Fermi-gas part). Values slightly below 10 MeV are obtained. The matching condition also determines a scaling factor for the Fermi-gas part. It is related with the collective enhancement of the level density. The corresponding results are shown by the red full lines. The transformation of the neutron-energies into the laboratory frame was performed considering the acceleration phase [55, 56] after scission by a numerical trajectory calculation.

The rather good reproduction of the measured neutron spectra, especially in the whole lower-energy part, does not give indication for neutron emission at scission [57, 58, 59, 60] although it is difficult to draw a definite conclusion due to the uncertainties in the level densities.

Simplified calculations show the importance of the emission during the acceleration phase. The

latter effect is stronger for the system ^{252}Cf(sf), since higher excitation energies and, thus, shorter emission times are involved in this system. Neutron emission during fragment acceleration reduces especially the laboratory energies of the first neutrons emitted at short times from the most highly excited fragments in ^{252}Cf(sf) and allows for a decently consistent description of the two systems with the GEF code, using the same parameter set.
Experimental prompt-fission neutron spectra of the systems $^{239}Pu(n_{th},f)$ and ^{240}Pu(sf) are compared with the result of the GEF code in figures 11 and 12, again using the same model parameters. Obviously, the data are very well reproduced.

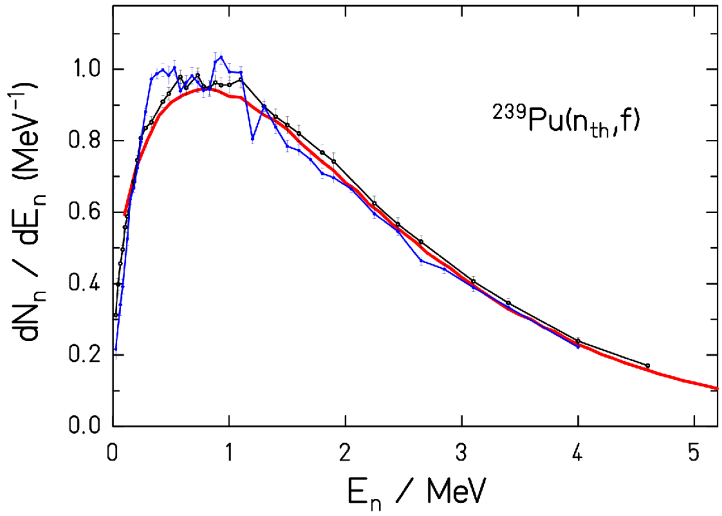

Figure 11. *Experimental prompt-fission-neutron spectrum for the system $^{239}Pu(n_{th},f)$ from ref. [61] (black open symbols) and from ref. [62] (blue full symbols) in comparison with the result of the GEF code (red thick full line). The calculated spectrum was normalized to the measured total neutron multiplicity ($\bar{\nu}=2.88$ [44]) by a factor of 1.025. The measured spectra are slightly scaled for minimizing the overall deviations from the calculated spectrum in order to better compare the spectral shapes.*

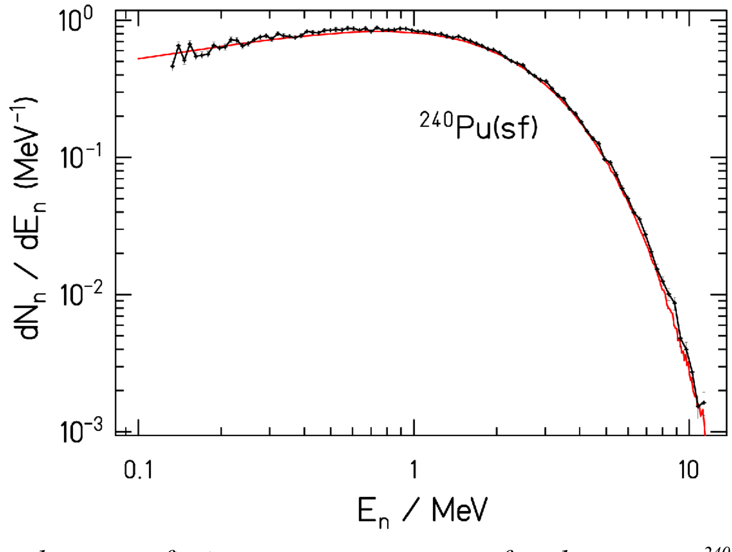

Figure 12. *Experimental prompt-fission-neutron spectrum for the system ^{240}Pu(sf) from ref. [63] (black symbols) in comparison with the result of the GEF code (red line). The measured data were scaled to the height of the calculated spectrum. Since the experiment covers especially well the lower-energy range, a double-logarithmic presentation was chosen.*

In general, the GEF code reproduces the available experimental fission-prompt-neutron spectra rather well. This qualifies the GEF code for estimating prompt-neutron spectra in cases where experimental data do not exist. The results of the GEF code for thermal-neutron-induced fission of several target nuclei are listed in the appendix. More data can be generated by downloading the code [8] and by performing the calculations with the appropriate system. The code also seems to be a suitable tool for improving evaluations.

Conclusion

The semi-empirical fission model, implemented in the GEF code, reproduces a large variety of observables with a good precision in a consistent way without further adjustment to specific fissioning systems with a unique parameter set. With this global approach one is able to predict several characteristic quantities of the fission process, e.g. the energy and multiplicity distribution of prompt-fission neutrons, without the need for specific experimental information of the respective system, e.g. measured mass-TKE distributions. All properties of the fission fragments that are considered in the code (e.g. nuclear charge, mass, excitation energy, angular momentum) are sampled in the corresponding multi-dimensional parameter space by a Monte-Carlo technique. Thus, all respective correlations are preserved. Moreover, correlations between all observables considered in the code are provided on an event-by-event basis.

Part of this work has been supported by the NEA of the OECD (http://www.oecd-nea.org/) and by the EFNUDAT (http://www.efnudat.eu/) and by the ERINDA (http://www.erinda.org/) projects of the European Union.

Appendix 1:

Table of prompt-neutron energy spectra for selected target nuclei in thermal-neutron-induced fission from a GEF calculation with 10^6 events. (ZT, AT: Z and A of target nucleus, nu: mean prompt-neutron multiplicity.)

ZT	90	90	90	90	90	90	91	91	91	91	91	91	92	92	92	92
AT	227	228	230	229	232	231	229	230	231	232	233	234	232	233	234	235
nu	1.921	1.753	1.815	1.876	1.793	1.960	1.899	2.180	1.972	2.189	2.045	2.215	2.191	2.440	2.185	2.391
E/MeV																
0.1	45567	44136	48409	48419	54471	52245	43303	48995	46177	51161	49410	53950	47498	52123	48635	53473
0.2	55211	53885	58648	59069	64739	63258	53047	60354	56105	63256	60116	66101	58028	64691	59034	65552
0.3	62034	59264	64742	64501	69053	69432	58581	67178	62214	69492	66507	72799	64816	72232	66151	73268
0.4	66187	62692	67552	68719	72114	72575	62113	71712	66007	74138	70627	77145	69160	76943	70572	77461
0.5	68603	65463	69339	71104	72645	75453	64869	75138	68770	77117	73697	80211	71984	80616	73100	81184
0.6	70176	66017	70446	72031	72794	76500	66386	76982	70359	78533	74762	81958	73617	82706	74993	83272
0.7	70191	66446	70309	71852	72078	76144	67231	77871	70832	78928	74639	81623	74815	83365	75944	83672
0.8	70692	65592	69785	70815	69782	75187	66781	77298	70986	79039	74134	81545	75190	83557	75563	83119
0.9	69169	63987	67719	69440	68304	73540	65891	76333	69350	78367	73053	80128	73983	82763	74784	83022
1	67631	62395	66039	67874	65302	71285	65065	75375	68506	76486	71816	78652	72563	81529	73786	81282
1.1	66102	60971	63307	65561	62803	69295	63117	73619	66720	74109	69520	76096	71095	80424	72299	79716
1.2	64576	58438	61562	63348	60529	66821	61626	71722	64452	72092	67554	74338	70088	78835	70675	78037
1.3	62187	56543	58719	60908	57893	64179	59904	70298	62645	70546	65693	71544	68428	76472	68423	75874
1.4	59672	54605	56177	58245	54815	61030	57435	67301	60418	68269	62819	69059	66583	73943	66291	73135
1.5	57344	52143	54008	55842	52334	58793	56212	64991	58358	65796	60841	66162	64426	71760	64272	70415
1.6	55731	50138	51420	53396	49659	55941	53953	62781	55718	62710	58189	63389	61521	69162	61813	67778
1.7	52418	47384	49007	50812	47027	53142	51778	60183	53587	59758	55618	60520	59367	66330	59593	65256
1.8	50027	45112	46319	48652	44542	50119	49530	57216	51386	57498	53050	57088	57056	63317	56835	62433
1.9	47790	43145	43727	45812	42095	47455	47484	55193	48632	54811	50581	54512	54945	60728	53865	59678
2	45570	40155	41655	43634	39637	45115	44966	52003	46543	52199	48061	51617	52457	58309	51934	56735
2.1	43104	38386	38914	41086	37285	42308	43016	50173	44393	49176	45689	49211	49812	55742	49187	53865
2.2	41149	36212	36995	38729	34860	39928	40456	47112	41703	46766	43422	46549	47462	53069	47056	51076
2.3	38287	34348	34667	36375	32776	38005	38769	44726	39984	44055	40916	43660	44921	50793	44625	48915
2.4	36618	32400	32491	34386	30917	35337	36503	42130	37529	41547	38269	41873	42869	48276	42125	45762
2.5	34505	30415	30408	32456	28964	33469	34978	39775	35236	39446	35966	39143	40954	45312	40103	43657
2.6	32056	28541	28810	30501	27160	31062	32858	37635	33350	37103	34058	36885	38562	42940	37859	41433
2.7	30313	26786	27108	28448	25529	29311	30642	35542	31624	35169	32333	34945	36710	40935	35988	39023
2.8	28560	25253	25353	26671	23927	27514	29059	33611	30109	33205	30504	32595	34556	38094	33817	36935
2.9	27074	23834	23800	24683	22307	25647	27590	31271	28059	30933	28625	30746	32539	36267	31986	34853
3	25359	22044	22570	23564	21106	24481	25863	29847	26378	29124	27072	28849	30819	34188	30529	32858
3.1	23608	20650	21058	21900	19452	22395	24585	27725	25006	27402	25258	27198	29066	32370	28596	30766
3.2	22117	19456	19682	20841	18450	21046	23079	26134	23338	25777	23805	25679	27541	30272	26745	29086
3.3	20820	18377	18227	19072	17150	19575	21680	24624	21856	24088	22349	23881	25709	28738	25293	27489
3.4	19628	17098	17046	17829	16135	18316	20294	22971	20717	22765	20527	22135	24229	27033	23687	25839
3.5	18224	16127	16096	16853	14670	17191	18961	21372	19382	21410	19740	20748	22825	25349	22572	24033
3.6	17124	15034	14824	15697	14113	15921	17767	19997	18156	19857	18482	19632	21431	23958	21153	22642
3.7	15768	13989	14006	14639	12972	14958	16821	19135	17077	18580	17105	18342	20046	22462	19899	21139
3.8	15025	12924	13164	13668	12359	14112	15647	17837	15832	17400	15912	17155	18756	21010	18321	19963
3.9	14031	12335	12084	13021	11464	12888	14757	16424	14893	16144	14960	16152	17848	19877	17407	18661
4	13102	11664	11253	11841	10562	11960	13751	15431	14106	15201	14073	15004	16680	18420	16135	17571
4.1	12059	10699	10657	11218	9959	11186	12936	14673	13110	14195	13047	13820	15818	17260	15127	16553
4.2	11534	10016	10033	10436	9108	10519	11953	13664	12077	13447	12153	13028	14594	16036	14114	15511
4.3	10422	9212	9325	9717	8653	9731	11119	12736	11365	12385	11401	11958	13599	15145	13298	14314
4.4	9766	8771	8686	8977	8059	9165	10454	11885	10744	11527	10616	11289	12998	14214	12395	13449
4.5	9055	7963	8080	8431	7463	8591	9647	10885	10051	10624	9736	10430	12201	13100	11819	12577
4.6	8572	7340	7496	7722	6792	7850	9171	10345	9381	9987	9190	9615	11184	12429	10865	11632
4.7	8040	7054	7037	7278	6385	7390	8666	9581	8675	9294	8528	9136	10678	11470	10097	10759
4.8	7408	6538	6426	6752	5998	6844	8092	8928	8052	8718	7904	8496	9862	10753	9603	10163
4.9	6972	6185	6024	6216	5650	6502	7463	8470	7440	8188	7476	7884	9274	10009	8950	9463
5	6349	5746	5676	5904	5283	5801	6885	7701	7004	7456	6947	7340	8458	9425	8171	9015
5.1	5892	5256	5336	5462	4956	5567	6574	7110	6566	7098	6519	6814	7854	8769	7869	8295
5.2	5600	4951	4949	5137	4509	5110	6038	6556	6103	6384	6051	6215	7420	8216	6993	7730
5.3	5301	4674	4588	4752	4243	4599	5568	6128	5628	5994	5651	5875	6972	7510	6774	7188
5.4	4986	4322	4325	4453	3840	4420	5244	5773	5275	5663	5280	5491	6575	7201	6364	6627
5.5	4432	4090	3864	3994	3606	4193	4919	5297	4806	5091	4760	5099	6050	6482	5827	6208
5.6	4077	3779	3627	3717	3344	3795	4557	4771	4522	4880	4588	4609	5567	6175	5413	5852
5.7	3923	3545	3396	3553	3142	3446	4174	4363	4257	4452	4126	4421	5092	5750	5093	5455
5.8	3630	3277	3164	3341	2839	3320	4071	4294	3950	4232	3875	4020	4889	5324	4754	5105
5.9	3285	2994	2839	3058	2680	2955	3603	3859	3625	3836	3737	3825	4634	5015	4379	4703
6	3102	2658	2727	2761	2402	2841	3412	3740	3381	3650	3367	3508	4353	4599	4014	4448
6.1	2811	2585	2524	2641	2309	2653	3197	3424	3150	3263	3183	3307	3914	4307	3764	3990
6.2	2615	2506	2313	2440	2142	2456	3011	3156	2942	3006	2924	3021	3566	4006	3583	3774
6.3	2460	2232	2075	2262	1951	2313	2709	2933	2793	2868	2746	2847	3297	3771	3269	3421
6.4	2302	2034	2037	2029	1931	1972	2575	2788	2531	2614	2531	2630	3165	3396	3064	3237
6.5	2211	1951	1819	1905	1692	1936	2309	2424	2376	2555	2335	2415	2955	3195	2828	3123
6.6	1983	1794	1747	1763	1579	1803	2179	2373	2126	2275	2192	2224	2659	3072	2671	2725
6.7	1854	1633	1688	1700	1475	1731	2048	2170	2085	2062	2004	2038	2529	2790	2445	2598
6.8	1659	1545	1468	1617	1297	1529	1922	1969	1838	1941	1966	1928	2352	2627	2275	2441
6.9	1535	1390	1358	1359	1234	1487	1703	1845	1767	1773	1807	1810	2230	2395	2111	2153
7	1462	1391	1228	1270	1089	1318	1567	1699	1702	1645	1536	1599	2046	2138	1959	2183
7.1	1330	1214	1144	1235	1036	1143	1462	1557	1457	1585	1488	1537	1929	2117	1892	1911
7.2	1243	1139	1066	1064	1001	1160	1463	1465	1423	1403	1435	1431	1733	1969	1758	1886
7.3	1127	1036	1070	1085	884	1017	1290	1365	1325	1390	1355	1315	1643	1848	1622	1624
7.4	1043	968	940	990	864	935	1198	1325	1144	1256	1179	1197	1515	1660	1510	1623
7.5	958	851	839	906	768	850	1038	1183	1131	1184	1044	1108	1391	1592	1438	1377
7.6	905	846	719	802	678	859	1047	1130	1030	1004	1006	1036	1298	1379	1278	1336
7.7	909	771	703	731	674	766	970	1007	999	970	1009	1013	1189	1323	1182	1240
7.8	816	738	691	724	566	711	889	950	919	889	915	915	1093	1177	1131	1091
7.9	724	655	589	636	513	613	827	864	814	837	781	821	1049	1131	1020	1050
8	682	621	597	569	521	607	750	755	728	762	783	703	1004	1099	959	1016
8.1	606	563	526	532	480	551	752	705	725	713	710	730	920	1018	901	989
8.2	603	539	535	472	475	561	643	669	659	672	691	631	822	926	778	797
8.3	526	438	421	471	428	446	657	638	597	608	601	587	763	830	692	867
8.4	504	441	396	442	382	402	566	540	565	601	563	546	680	747	721	782
8.5	444	440	371	444	354	405	490	523	553	510	500	515	710	728	703	653
8.6	402	383	384	371	351	342	451	516	504	484	451	474	606	649	640	656
8.7	423	375	311	338	290	340	468	483	455	456	466	447	606	638	583	554
8.8	324	323	323	348	252	334	403	412	410	417	404	384	509	576	544	518
8.9	301	307	290	307	251	285	366	396	400	398	351	347	487	512	480	504
9	296	266	277	274	216	286	327	392	376	390	353	391	474	489	443	489
9.1	271	257	225	263	237	227	314	379	319	308	319	316	427	481	428	436
9.2	251	217	207	221	208	227	298	304	316	316	289	310	389	449	425	434
9.3	233	194	194	208	201	213	267	273	280	291	262	292	374	470	345	375
9.4	219	216	188	218	153	197	298	261	266	275	267	263	334	373	317	383
9.5	188	208	156	179	147	170	257	247	251	237	240	247	334	377	297	335
9.6	184	187	162	149	131	167	244	237	210	221	229	224	318	300	323	290
9.7	183	168	154	143	125	144	204	213	201	223	197	201	274	275	301	264
9.8	176	155	174	117	136	144	173	207	217	184	194	185	270	264	259	248
9.9	169	130	129	143	130	136	203	190	194	157	200	172	217	278	220	243
10	120	125	105	118	83	126	174	143	170	160	147	182	217	260	227	244

ZT	92	92	92	92	93	93	93	93	93	93	94	94	94	94	94	94
AT	236	237	238	239	234	235	236	237	238	239	236	237	238	239	240	241
nu	2.288	2.472	2.411	2.559	2.661	2.411	2.692	2.469	2.771	2.572	2.718	2.965	2.755	3.024	2.819	3.112
E/MeV																
0.1	52092	56430	56462	59992	54079	50381	55811	52169	58719	55884	54305	58862	55878	60667	57948	63220
0.2	63613	68922	68020	73023	67054	61504	69372	64279	72714	68154	67088	73405	68784	75459	71015	78299
0.3	70683	76826	76210	81279	74725	68473	77899	71827	80913	76041	75028	81653	76650	85145	79623	87480
0.4	75241	81766	80928	86675	81025	73654	83496	76346	86541	80885	80540	87932	82237	91131	84652	94059
0.5	78323	84262	84019	89964	84639	76334	87409	79393	90336	84406	84039	92185	85621	94507	88506	98194
0.6	80023	86478	85029	91455	86555	78906	89669	81447	93415	86059	86104	95323	87940	97529	91060	101824
0.7	80397	87734	86140	91891	87858	79179	91241	82772	94045	87565	87826	96759	88518	99375	92047	102552
0.8	80472	87508	85858	91936	88395	79549	91146	82734	94375	87160	87880	97621	89892	99694	92161	102234
0.9	78953	86035	84644	90211	88586	79373	90667	81881	93683	86528	88273	96950	89061	99893	92655	102592
1	78001	84424	83332	88619	87364	78785	89772	81285	92712	85689	86853	97127	88534	98820	90346	101109
1.1	75597	82636	80636	86604	86387	77176	88477	79954	90521	84591	85676	94163	87936	96662	89422	99547
1.2	73837	80634	78950	84472	84728	75782	86126	77912	88990	81605	84302	93024	85681	95032	88408	97638
1.3	71831	78211	76490	81535	82360	73362	84276	76361	86627	80254	82206	90340	83771	93720	86319	95060
1.4	69713	75293	73927	78318	80713	71789	81540	73421	84853	77638	80085	88687	81727	90900	83125	93280
1.5	67345	72939	70747	75885	78541	69569	79593	71413	81646	74777	78072	86449	79493	87789	81654	90532
1.6	64510	70498	68612	72552	74913	67484	76307	68900	78312	72697	75739	83289	76365	85002	78945	87216
1.7	61825	67343	65248	69726	72511	65035	74099	66628	75632	68939	72972	80848	74064	81860	75797	84313
1.8	59469	63865	62255	66232	69753	62299	70427	63926	72745	66546	70664	77702	71822	79252	73122	80748
1.9	56936	61505	60328	63092	66821	60111	68040	60898	69326	63856	67604	74010	68512	75532	70332	77698
2	54202	58010	57063	60599	64207	57285	64998	58736	66306	60948	64735	71778	65693	72902	66965	74450
2.1	51318	55885	53928	57230	61226	55389	61652	55951	63319	58206	62602	68643	62851	70104	64189	71777
2.2	49174	52506	51321	54333	58625	52431	58902	53507	60146	55664	60175	65244	60398	66537	61599	67899
2.3	46524	50099	48600	51526	55948	49568	55804	50879	57372	52792	56434	62150	57533	63236	59018	65113
2.4	44163	47586	46001	48812	53861	47613	53044	48333	54720	49999	54610	59804	54911	60090	56008	61624
2.5	41372	44931	43642	45841	50604	45211	50142	46016	51583	47729	51688	56331	52389	57466	53115	59242
2.6	39191	42429	41335	43387	47951	43399	48153	43924	48958	44967	49361	54223	49828	54272	50509	55652
2.7	37455	40044	38582	40781	45343	41023	45371	41305	46164	42673	46675	51072	47339	51717	48078	53207
2.8	35204	37995	36645	38394	43135	38742	42942	39363	43859	40332	44684	48592	44847	48970	45952	50761
2.9	33213	35565	34392	36121	40846	36516	40653	37514	41913	38467	42255	45794	42503	46717	43006	47895
3	31174	33493	32487	34176	38389	35009	38030	35148	39148	36261	40070	43222	40155	43751	41044	45253
3.1	29523	31707	30689	32259	36623	33043	36239	33226	36670	33964	37865	40910	38141	41595	38764	42434
3.2	27800	29983	28736	30285	34334	31066	34126	31589	35081	32226	35882	38496	36129	38960	36743	40250
3.3	25781	28166	27047	28012	31949	29301	32193	29643	32705	30150	33546	36849	34041	36973	34427	37706
3.4	24423	26220	25321	26899	30112	27449	30358	27766	30682	28257	32050	34818	32459	34949	32357	35987
3.5	23239	24609	24040	25130	28885	26018	28200	26532	29023	26834	30130	32293	30451	32651	30665	33876
3.6	21415	22998	22224	23583	26737	24762	26397	24486	27122	25217	28404	30302	28607	31237	28888	31528
3.7	20281	21984	20832	21824	25114	23327	24748	23354	25529	23906	27206	28914	26601	29113	27586	29873
3.8	19003	20605	19409	20747	23888	21953	23524	21950	24043	22346	25033	27076	25227	27207	25738	28062
3.9	17840	19113	18020	19078	22364	20456	21922	20852	22434	20986	23939	25247	23761	25764	24039	26505
4	16737	17760	16910	18020	20956	19234	20599	19348	20928	19719	22088	24199	22532	24251	22853	24797
4.1	15477	16719	15962	16773	19604	18179	19369	18498	19612	18468	20947	22566	21038	22780	21185	23268
4.2	14558	15466	14955	15787	18624	16716	18226	16951	18692	17232	19632	21110	19794	21408	20057	21837
4.3	13681	14625	14118	14870	17222	15895	16997	15888	17333	16170	18426	19807	18608	19859	18640	20522
4.4	13205	13744	13158	13665	15891	14589	15956	14997	16096	15339	17428	18331	17164	18638	17826	19317
4.5	11893	12732	12106	12805	14979	13954	14778	14155	15049	14334	16336	17392	16419	17592	16370	18031
4.6	11193	12063	11447	12073	14107	12975	13837	13023	14335	13369	15003	16452	15520	16244	15428	16751
4.7	10497	11102	10627	11130	13162	12049	13011	12293	13434	12551	14224	15061	14148	15249	14442	15878
4.8	9762	10484	9821	10345	12468	11489	12035	11532	12411	11627	13511	14178	13476	14318	13460	14547
4.9	8942	9783	9255	9730	11590	10807	11348	10628	11681	10881	12357	13231	12645	13327	12675	13886
5	8595	9032	8706	8956	10800	10151	10670	10006	10619	10103	11681	12478	11766	12203	11750	12951
5.1	7932	8383	8180	8291	10204	9344	9829	9535	10067	9449	10862	11679	11124	11600	11252	11884
5.2	7352	7944	7343	7962	9448	8784	9222	8711	9261	8768	10178	10778	10318	10968	10303	11292
5.3	6699	7364	6993	7201	8742	8059	8664	8078	8877	8218	9579	10010	9513	10176	9700	10493
5.4	6311	6908	6471	6715	8158	7511	7964	7695	8272	7695	8963	9247	8992	9596	9172	10023
5.5	5994	6399	6056	6279	7676	7174	7413	7103	7533	7126	8374	8669	8333	8967	8321	9167
5.6	5648	5965	5560	5728	7052	6653	6852	6657	7087	6821	7900	8252	7845	8320	7746	8608
5.7	5316	5369	5243	5555	6614	6135	6480	6238	6842	6188	7237	7553	7241	7655	7426	8002
5.8	4783	5009	4966	5047	6176	5707	5971	5858	6204	5868	6877	7029	6775	7247	7005	7499
5.9	4459	4673	4560	4680	5598	5523	5465	5396	5725	5530	6329	6670	6383	6721	6518	6985
6	4067	4491	4178	4446	5494	4964	5110	5007	5323	5129	5830	6115	5852	6140	5939	6607
6.1	3870	4073	3890	4189	4997	4761	4817	4736	4973	4766	5732	5781	5562	5948	5588	5945
6.2	3585	3802	3614	3812	4537	4444	4640	4362	4571	4431	5105	5354	5119	5484	5192	5583
6.3	3370	3525	3387	3512	4297	4094	4279	4135	4302	4055	4690	4971	4891	5060	4863	5297
6.4	3107	3329	3122	3259	3868	3855	3821	3794	3917	3881	4461	4680	4520	4720	4524	4939
6.5	2820	3094	2954	3012	3682	3695	3586	3612	3705	3518	4277	4374	4207	4456	4263	4529
6.6	2704	2920	2799	2806	3433	3293	3343	3292	3467	3294	3819	3992	3857	4058	3951	4305
6.7	2534	2681	2459	2559	3231	3103	3085	3077	3176	3229	3636	3793	3678	3807	3574	3976
6.8	2269	2453	2370	2458	3027	2924	2885	2948	2971	2909	3410	3572	3481	3525	3358	3635
6.9	2192	2293	2230	2273	2810	2723	2764	2685	2755	2730	3211	3306	3039	3267	3196	3411
7	2033	2095	2021	2155	2611	2444	2510	2378	2572	2523	2879	3036	2962	3083	2882	3139
7.1	1940	2028	1842	2015	2349	2376	2301	2398	2366	2329	2821	2739	2785	2845	2749	3080
7.2	1756	1748	1726	1808	2221	2149	2221	2125	2231	2203	2556	2652	2494	2683	2590	2728
7.3	1577	1724	1675	1742	2063	1916	1934	2019	2147	1934	2398	2425	2345	2547	2401	2477
7.4	1450	1705	1516	1519	1843	1801	1910	1861	1882	1873	2184	2179	2279	2293	2216	2412
7.5	1407	1480	1335	1439	1720	1700	1721	1735	1744	1706	2088	2103	2093	2041	2063	2211
7.6	1258	1387	1273	1305	1589	1582	1576	1635	1705	1668	1859	1948	1863	1954	2026	2134
7.7	1214	1225	1211	1273	1555	1493	1525	1502	1473	1480	1690	1754	1814	1868	1808	1818
7.8	1187	1212	1179	1214	1412	1406	1382	1421	1432	1408	1669	1733	1753	1723	1754	1765
7.9	1046	1090	1055	1014	1358	1317	1300	1294	1285	1304	1540	1628	1553	1603	1562	1648
8	915	978	946	967	1247	1213	1179	1228	1216	1221	1540	1540	1512	1450	1432	1585
8.1	949	932	818	890	1154	1153	1118	1104	1164	1121	1303	1310	1373	1402	1360	1473
8.2	899	895	861	896	1111	1024	1016	1064	1074	995	1231	1264	1255	1262	1275	1359
8.3	741	840	745	779	992	969	959	966	953	914	1206	1165	1202	1231	1218	1139
8.4	725	743	727	790	938	904	843	917	961	909	1078	1038	1098	1058	1077	1233
8.5	643	707	670	655	883	807	810	833	911	834	1002	1061	996	1022	1041	1086
8.6	601	665	645	630	750	742	780	788	838	800	945	969	955	942	915	994
8.7	579	658	586	627	704	728	694	694	723	715	863	911	912	886	904	978
8.8	577	545	552	558	657	705	636	656	659	668	819	802	853	839	823	936
8.9	511	526	484	532	669	623	594	663	647	640	810	696	790	757	794	822
9	442	486	451	508	588	563	622	589	599	571	720	699	751	709	658	788
9.1	437	469	435	422	547	550	538	549	544	563	679	639	688	673	652	674
9.2	374	379	408	420	471	507	470	554	544	495	604	590	604	635	653	658
9.3	370	391	368	361	483	488	475	455	484	461	529	604	545	599	591	566
9.4	329	356	354	360	442	443	401	456	497	457	490	537	526	536	530	558
9.5	310	334	314	341	401	370	401	369	425	409	485	453	522	512	501	555
9.6	328	318	293	296	381	395	378	379	420	398	483	488	472	486	475	499
9.7	256	272	277	286	344	357	313	339	350	348	440	456	460	437	427	457
9.8	262	272	276	270	325	333	274	343	342	331	399	401	430	420	414	449
9.9	210	245	234	244	315	254	316	272	296	301	347	366	387	396	416	415
10	218	231	246	245	270	268	273	276	255	286	344	333	331	364	369	366

ZT	94	94	95	95	95	95	95	95	96	96	96	96	96	96	96	96
AT	242	243	239	240	241	242	243	244	242	243	244	245	246	247	248	249
nu	2.943	3.241	3.027	3.244	3.052	3.344	3.159	3.465	3.370	3.594	3.402	3.701	3.494	3.805	3.579	3.909
E/MeV																
0.1	61005	67397	58774	62525	60568	65190	63507	68752	64631	68250	65725	71466	69084	74742	72263	78028
0.2	75171	82789	72628	77933	74228	81346	77857	86102	79772	84687	81222	88534	84812	92418	88472	96891
0.3	83691	92815	80807	86793	82987	90732	86723	96376	89055	95829	90743	98788	95269	104471	98436	107998
0.4	88996	98998	86764	93886	88560	98120	92810	103663	95019	101819	97113	106507	101242	111986	105736	115998
0.5	93058	103240	91165	98360	93216	102857	97485	108696	99398	107289	102202	112283	105827	117324	110312	121733
0.6	95674	106786	93198	101476	95716	105465	100255	112481	102533	111077	104628	115476	109322	121299	112692	125210
0.7	96813	108609	95727	103131	96741	107506	102018	113435	104799	112693	106565	117563	110368	122731	114547	126488
0.8	97003	108060	95943	104528	97736	107851	101635	115134	106225	113524	107753	118697	111045	123284	115442	128508
0.9	95956	107807	96154	104157	97913	108216	101394	114487	105772	113908	107069	118270	111049	123193	114986	127883
1	95511	106413	94272	103982	96934	107309	101063	113577	105136	113218	106322	118160	110199	123024	113707	126477
1.1	94115	105146	93717	102222	95154	105572	99097	112234	103989	112994	105179	117143	109028	120522	112371	124246
1.2	92638	102645	92945	100177	93417	103927	97851	109808	101957	110821	103850	114956	107480	119731	110777	122964
1.3	90108	100487	90674	98373	92106	101620	95157	107441	100416	108378	101378	112118	104617	116322	107972	120008
1.4	88017	97460	88602	96235	89303	99939	92869	104020	98627	105946	99759	109513	101734	113161	105881	116446
1.5	85045	94822	86253	93551	87417	96500	90233	101077	96231	103176	97009	107014	99942	109733	102740	112949
1.6	82727	92101	84029	90779	84161	93535	88056	98180	92927	100729	93764	103512	97224	106882	99392	109572
1.7	79453	88360	81048	87444	81638	90413	84923	94415	89717	97053	91515	99938	93794	102828	96105	106433
1.8	76129	85139	77949	85025	78597	87892	81970	90818	86979	94005	87714	96428	90549	99074	92250	102409
1.9	73525	81137	75421	82029	75534	84100	78120	87030	84087	90376	84625	92952	86987	96306	89118	98326
2	70067	77670	72486	78364	73327	80778	75259	83607	80598	86613	81487	88972	83061	91814	85298	93697
2.1	67104	74530	69708	74770	69754	76364	73002	80041	77945	83134	78616	85548	79702	88066	82287	90572
2.2	65143	70485	66659	71729	67023	74038	69095	76294	74259	79691	74563	81497	77293	83618	78639	86514
2.3	60997	67306	63683	68722	64143	71070	66491	73096	71274	75899	71464	78556	73710	80046	74852	81908
2.4	58426	64378	61121	65515	61133	67752	62372	69149	68163	72690	68685	74076	69809	76356	71848	78043
2.5	55363	60807	58224	62115	58629	63819	60212	66150	64724	69004	65532	71437	66479	73259	67849	74197
2.6	52641	57850	55044	59576	55482	60622	57137	62657	62157	66307	62526	67649	63904	69176	65100	70794
2.7	49718	55199	52914	56670	52699	57513	54384	59365	59541	62953	58980	64518	60854	65962	61152	67156
2.8	47426	52166	50335	53809	49934	54920	51777	56126	56138	60161	56737	60788	57645	62771	58795	63867
2.9	44749	49568	47908	51210	47800	52320	48578	53041	53485	56796	53875	58010	54820	59139	55237	60685
3	42487	46444	45445	48338	45335	49426	46489	50588	50638	54179	51445	54764	51889	55865	53096	57271
3.1	39730	43222	42673	45423	42582	46978	43896	47099	47945	51028	48327	51956	49011	53311	49903	54211
3.2	38054	41319	40633	43433	40454	44127	41293	45178	45691	48155	46076	49617	46186	50017	46795	51217
3.3	35720	38722	38541	40639	38310	41814	39461	42157	42824	45738	43333	46294	43943	47057	44824	48238
3.4	33897	36508	36473	38363	36265	39588	37639	39926	40848	43234	40966	43921	41715	44483	42190	45163
3.5	31928	34675	34219	36358	34376	37283	35070	37661	38646	40603	38525	41380	38988	42098	39661	42936
3.6	30083	32446	32117	34303	32606	35108	33042	35364	36445	38785	36790	39039	37100	39738	37413	40757
3.7	28315	30885	30656	32230	30487	32936	31507	33344	33964	36568	34430	36883	35163	37546	35112	37842
3.8	26156	28762	28826	30795	28491	31051	29381	31242	32314	33931	32427	34638	33033	34944	33228	35815
3.9	25081	27095	27133	28455	27178	28982	27762	29414	30797	32156	30474	32710	30969	32744	31432	33401
4	23329	25507	25509	27123	25566	27790	26054	27673	28828	30119	28665	30761	29271	30656	29279	31300
4.1	22106	23876	24234	25153	23862	25876	24509	25993	27310	28861	27035	28909	27523	28870	27619	29455
4.2	20597	22127	22378	23661	22598	24200	23038	23909	25584	26915	25536	27300	25533	27170	25802	27769
4.3	19266	20958	21322	22146	21486	22760	21729	22653	23993	25087	23947	25550	24342	25644	24388	25820
4.4	18165	19582	20317	20808	19751	21491	20321	21150	22388	23662	22628	23923	22728	24136	22834	24336
4.5	17120	18112	18668	19857	18788	19744	19060	19760	20997	22184	21047	22412	21261	22358	21453	22635
4.6	15957	16811	17402	18465	17657	18755	17878	18591	19725	20675	19721	20983	19958	20974	20018	21501
4.7	14813	15853	16493	17205	16616	17431	16633	17401	18813	19291	18551	19672	18810	19677	18939	19892
4.8	14043	15100	15479	16029	15396	16416	15844	16254	17640	17955	17574	18638	17581	18188	17744	18691
4.9	12943	13889	14741	15060	14436	15122	14408	15065	16656	16994	16274	17176	16534	17377	16616	17423
5	12128	12990	13566	14094	13298	14348	13500	14207	15376	16175	15299	16451	15617	16089	15703	16565
5.1	11483	12302	12757	13280	12642	13342	12928	13220	14098	14924	14457	14976	14467	15065	14341	15144
5.2	10816	11294	11787	12329	11593	12430	12050	12349	13229	14059	13382	14331	13570	14084	13524	14339
5.3	10116	10527	11084	11543	11167	11695	11192	11468	12749	13018	12517	13412	12786	13031	12715	13427
5.4	9064	9973	10404	10594	10407	10904	10515	10704	11716	12139	11698	12466	11782	12280	11773	12458
5.5	8635	9327	9774	10146	9647	10210	9831	10080	11049	11524	10975	11612	11122	11324	11180	11551
5.6	8188	8538	9162	9434	9008	9569	8997	9243	10463	10594	10331	10977	10205	10757	10436	10685
5.7	7668	8054	8639	8765	8564	8942	8551	8666	9876	9970	9570	9925	9829	10037	9631	10208
5.8	7022	7426	7969	8208	7757	8273	7940	8025	9062	9313	9027	9381	9045	9410	8852	9499
5.9	6704	6918	7470	7701	7548	7710	7621	7499	8525	8864	8361	8618	8503	8815	8521	8714
6	6126	6570	7025	7096	6928	7270	6875	6980	8002	8182	7944	8213	7926	8071	7826	8241
6.1	5820	6065	6554	6606	6400	6766	6509	6639	7446	7652	7412	7735	7598	7610	7302	7827
6.2	5330	5577	6152	6207	6098	6290	6073	6083	6892	7105	6870	7230	6825	7158	6815	7012
6.3	5000	5242	5716	5893	5533	5880	5660	5764	6484	6712	6473	6642	6596	6561	6484	6605
6.4	4614	4925	5381	5289	5323	5513	5326	5472	5980	6158	6036	6186	6020	6193	5952	6130
6.5	4372	4608	4841	5028	4887	4944	4984	4927	5663	5694	5503	5797	5593	5656	5680	5897
6.6	4058	4285	4637	4710	4636	4755	4535	4668	5202	5421	5087	5497	5436	5389	5480	5424
6.7	3814	3999	4159	4282	4225	4506	4406	4291	4960	4968	4827	5101	4854	4927	4971	4997
6.8	3520	3625	4037	4098	3989	4040	4055	3982	4704	4628	4653	4669	4604	4732	4519	4626
6.9	3364	3486	3673	3885	3719	3848	3830	3584	4249	4192	4333	4417	4291	4437	4316	4348
7	3002	3246	3409	3522	3386	3605	3455	3456	3888	4011	4058	4155	4126	4090	4004	4153
7.1	3014	3008	3296	3235	3229	3309	3215	3307	3687	3878	3631	3770	3653	3779	3765	3727
7.2	2653	2721	2953	3002	2943	3127	2979	2979	3502	3606	3524	3600	3434	3478	3488	3571
7.3	2408	2523	2788	2852	2801	2925	2884	2844	3261	3155	3278	3250	3221	3220	3202	3337
7.4	2246	2296	2604	2797	2628	2530	2661	2610	2992	3067	3095	3110	3108	3033	3022	3059
7.5	2188	2200	2501	2433	2375	2536	2389	2462	2833	2829	2774	2869	2833	2837	2794	2881
7.6	2049	1984	2312	2207	2214	2337	2293	2341	2625	2686	2604	2733	2675	2673	2610	2676
7.7	1763	1941	2111	2123	2090	2171	2155	2162	2446	2503	2499	2537	2465	2476	2461	2507
7.8	1664	1799	2004	1946	1958	2059	2038	2047	2209	2291	2288	2318	2295	2412	2281	2351
7.9	1573	1741	1915	1932	1806	1960	1886	1875	2110	2175	2131	2157	2141	2153	2133	2176
8	1481	1539	1777	1699	1704	1780	1696	1684	1997	2067	2025	1989	2000	1934	2022	1980
8.1	1380	1425	1609	1524	1570	1706	1618	1561	1859	1911	1863	1855	1851	1801	1845	1906
8.2	1291	1339	1476	1443	1435	1486	1506	1496	1722	1803	1715	1768	1708	1697	1728	1790
8.3	1189	1280	1409	1380	1454	1388	1351	1345	1650	1549	1574	1629	1592	1604	1626	1613
8.4	1168	1127	1264	1315	1335	1318	1323	1237	1539	1510	1506	1482	1494	1550	1565	1559
8.5	1061	1078	1185	1282	1211	1210	1257	1194	1371	1413	1309	1460	1397	1397	1431	1450
8.6	980	1005	1070	1065	1099	1117	1124	1120	1317	1281	1342	1288	1266	1281	1330	1248
8.7	909	960	1052	1029	1042	1030	1108	1057	1279	1275	1214	1235	1240	1259	1274	1257
8.8	836	875	956	982	968	979	987	961	1167	1172	1089	1055	1060	1110	1192	1133
8.9	835	777	968	886	955	945	954	938	991	1079	1096	1107	1027	1039	1019	1087
9	740	804	852	838	840	867	849	828	949	975	1068	962	927	991	1001	981
9.1	746	711	848	766	854	806	801	808	959	914	935	963	927	864	905	903
9.2	631	636	758	741	723	716	763	707	855	883	876	902	872	843	865	851
9.3	587	621	686	715	669	741	744	643	832	803	794	830	758	770	776	736
9.4	558	574	651	651	625	620	615	598	766	726	748	766	784	795	724	745
9.5	514	542	606	625	600	631	590	566	649	683	670	712	685	692	696	681
9.6	461	504	618	571	557	596	534	533	650	682	673	687	649	569	651	692
9.7	444	477	519	539	530	520	515	493	606	581	624	640	619	636	579	578
9.8	407	467	437	499	514	496	526	486	573	567	587	557	560	564	579	576
9.9	390	422	456	453	429	452	486	418	523	482	503	566	555	487	524	524
10	373	351	449	383	425	451	428	395	507	488	466	469	491	497	494	477

1 K.-H. Schmidt, B. Jurado, JEF/DOC 1423, NEA of OECD, Paris, 2011, available from [8]
2 K.-H. Schmidt et al., Nucl. Phys. A 665 (2000) 221
3 M. G. Itkis et al., Sov. J. Nucl. Phys. 52 (1990) 601
4 A. N. Andreyev et al., Phys. Rev. Lett. 105 (2010) 252502
5 S. I. Mulgin, K.-H. Schmidt, A. Grewe, S. V. Zhdanov, Nucl. Phys. A 640 (1998) 375
6 J. P. Unik et al., Proc. Symp. Phys. Chem. Fission, Rochester 1973, IAEA Vienna (1974), vol. 2, p. 19
7 B. D. Wilkins, E. P. Steinberg, R. R. Chasman, Phys. Rev. C 14 (1976) 1832
8 http://www.cenbg.in2p3.fr/GEF, http://www.khs-erzhausen.de
9 I. Ragnarsson, R. K. Sheline, Phys. Scr. 29 (1984) 385
10 M. Brack et al., Rev. Mod. Phys. 44 (1972) 320
11 U. Mosel, H. Schmitt, Phys. Rev. C 4 (1971) 2185
12 K.-H. Schmidt, A. Kelic, M. V. Ricciardi, Europh. Lett. 83 (2008) 32001
13 S. Panebianco, J.-L. Sida, H. Goutte, J.-F. Lemaître, N. Dubray, S.Phys. Rev. C 86 (2012) 064601
14 A. V. Karpov, P. N. Nadtochy, D. V. Vanin, G. D. Adeev, Phys. Rev. C 63 (2001) 054610
15 A. V. Karpov, G. D. Adeev, Eur. Phys. J. A 14 (2002) 169
16 H. Nifenecker, J. Physique Lett. 41 (1980) 47
17 B. Bouzid et al., J. Phys. G: Nucl. Part. Phys. 24 (1998) 1029
18 J. R. Nix, Ann. Phys. 41 (1967) 52
19 D. Bucurescu, T. von Egidy, Phys. Rev. C 72 (2005) 06730
20 L. Bonneau, P. Quentin, I. N. Mikhailov, Phys. Rev. C 75 (2007) 064313
21 F. Gönnenwein, I. Tsekhanovich, V. Rubchenya, Intern. J. Mod. Phys. E 16 (2007) 410
22 S. G. Kadmensky, Phys. Atom. Nuclei 71 (2008) 1193
23 H. Naik, S. P. Dange, R. J. Singh, A. V. R. Reddy , Eur. Phys. J. A 31 (2007) 195
24 L. G. Moretto, G. F. Peaslee, G. J. Wozniak, Nucl. Phys. A 502 (1989) 453c
25 H. Goutte, J. F. Berger, P. Casoli, D. Gogny, Phys. Rev. C 71 (2005) 024316
26 J. Randrup, P. Möller, A. J. Sierk, Phys. Rev. C 84 (2011) 034613
27 A. S. Jensen, T. Døssing , Proc. Symp. Phys. Chem. Fission, Rochester 1973, IAEA Vienna (1974), vol. 1, p. 40
28 A. V. Voinov et al., Phys. Rev. C 79 (2009) 031301
29 V. M. Kolomietz, S. Åberg, S. V. Radionov , Phys. Rev. C 77 (2008) 014305
30 U. Brosa, S. Grossmann, A. Müller, Phys. Rep. 197 (1990) 167
31 N. Dubray, H. Goutte, J.-P. Delaroche, Phys. Rev. C 77 (2008) 014310
32 A. A. Naqvi, F. Käppeler, F. Dickmann, R. Müller, Phys. Rev. C 34 (1986) 21
33 A. V. Voinov et al., Phys. Rev. C 79 (2009) 031301
34 M. Guttormsen et al., Phys. Rev. C 68 (2003) 034311
35 Y. Alhassid, G. F. Bertsch, L. Fang, Phys. Rev. C 68 (2003) 044322
36 G. G. Dussel, S. Pittel, J. Dukelsky, P. Sarriguren , Phys. Rev. C 76 (2007) 011302
37 K.-H. Schmidt, B. Jurado, Phys. Rev. Lett. 104 (2010) 21250
38 K.-H. Schmidt, B. Jurado, Phys. Rev. C 82 (2011) 014607
39 K.-H. Schmidt, B. Jurado, Phys. Rev. C 83 (2011) 061601
40 M. Caamaño, F. Rejmund, K.-H. Schmidt, J. Phys. G: Nucl. Part. Phys. 38 (2011) 035101
41 S. Steinhäuser et al., Nucl. Phys. A 634 (1998) 89
42 K.-H. Schmidt. B. Jurado, arXiv:1007.0741v1[nucl-th] (2010)
43 W. Lang et al., Nucl. Phys. A 345 (1980) 34
44 M. S. Zucker, N. E. Holden , Report BNL-38491 (1986)
45 R. Müller, A. A. Naqvi, F. Käppeler, F. Dickmann , Phys. Rev. C 29 (1984) 885
46 E. J. Axton, Nucl. Stand. Ref. Data (1985) 214.
47 N. V. Kornilov et al., Nucl. Science Engin. 165 (2010) 117.
48 W. Mannhart, INDC(NDS)-220/L (1989) 305, IAEA, Vienna.
49 J. R. Huizenga, R. Vandenbosch, Phys. Rev. 120 (1960) 130.
50 A. R. Junghans et al., Phys. Lett. B 670 (2008) 200.
51 T. von Egidy, D. Bucurescu, Phys. Rev. C 78 (2008) 05130.
52 A. V. Ignatyuk, G. N. Smirenkin, A. S. Tishin, Sov. J. Nucl. Phys. 21 (1975) 255.
53 A. V. Ignatyuk, Hadrons Nuclei Appl. 3 (2001) 287.
54 K..-H. Schmidt, B. Jurado, Phys. Rev. C 86 (2012) 044322
55 V. P. Eismont, Atomn. Ener. 19 (1965) 113.
56 V. M. Maslov et al., Eur. Phys. J. A 18 (2003) 93.
57 N. V. Kornilov et al., Nucl. Phys. A 686 (2001) 187.
58 G. V. Danilyan et al., Phys. Atom. Nucl. 71 (2008) 200.
59 G. A. Petrov et al., Phys. Atom. Nucl. 71 (2008) 1137.
60 N. Carjan. M. Rizea, Phys. Rev. C 82 (2010) 01461.
61 A. A.Bojcov et al., 6th All Union Conf. Kiev (1983) Vol. 2, p. 294.
62 A. Lajtai et al., Nucl. Data Conf., Santa Fe (1985) Vol. 1, p. 613.
63 L. V. Drapchinsky et al., communicated by N. Capote, 2012.